Mineralogical Magazine, June 2012, Vol. 76(3), pp. 761–767

Xenotime-(Y) and Sn-rich thortveitite in miarolitic pegmatites from Baveno, Southern Alps, Italy

A. Guastoni[1], F. Nestola[1,*], C. Ferraris[2] and G. Parodi[2]

[1] Department of Geosciences, University of Padova, Via Gradenigo 6, I-35131 Padova, Italy
[2] Laboratoire de Minéralogie et Cosmochimie Muséum National d'Histoire Naturelle, Rue Buffon 61, CP52, 75005 Paris, France

[*Received 21 February 2012; Accepted 17 May 2012; Associate Editor: Fernando Cámara*]

ABSTRACT

Xenotime-(Y), (Y,*REE*)PO_4, and thortveitite, $(Sc,Y)_2Si_2O_7$, in a miarolitic cavity in a niobium, yttrium, fluorine (NYF) granitic pegmatite at Baveno, Verbania, Southern Alps, Italy, were investigated by electron microprobe analysis and single-crystal X-ray diffraction. Fluorine has an important role as a complexing agent for Y and *REE*s in supercritical pegmatitic fluids; annite-siderophyllite and chamosite are the most likely sources of the Y and *REE*s. The thortveitite from Baveno contains up to 3.20 wt.% SnO_2, an unusually high Sn content. Xenotime-(Y) is enriched in Gd in comparison to other Alpine xenotimes. Quantitative chemical data and measurements of the lattice parameters show that a higher scandium content results in a smaller unit-cell volume in thortveitite. The substitution of *REE*s for Y up to ~20 mol.% has little effect on the unit cell of xenotime-(Y). The textures of xenotime-(Y) and thortveitite provide information about the dissolution and crystallization processes in the miarolitic cavity.

Keywords: Baveno, miarolitic cavities, NYF pegmatite, thortveitite, xenotime-(Y).

Introduction

Crystallization processes of accessory minerals which occur in miarolitic cavities support the role of water, fluorine and carbonate as complexing agents to transport incompatible elements at lower temperatures in silicate melts containing niobium, yttrium, fluorine (NYF) rare-element pegmatites (Wood, 1990; Gramaccioli *et al.*, 2000*b*; Pezzotta *et al.*, 2005; London, 2008; Guastoni and Nestola, 2010).

Crystal growth processes in pegmatites are controlled by factors including the kinetics of nucleation, diffusion and the selective adsorption of elements at fluid–crystal interfaces. These processes are primarily controlled by the saturation, temperature and pressure conditions. In particular, the degree of supersaturation, which controls the precipitation of incompatible elements in supercritical fluids and melts in pegmatitic systems, depends on undercooling temperatures and SiO_2 activity (David London, pers. comm.).

In this study we provide data on crystals of xenotime-(Y), (Y,*REE*)PO_4, and thortveitite, $(Sc,Y)_2Si_2O_7$, in a centimetre-sized miarolitic cavity from a granitic pegmatite at Baveno, Verbania, Southern Alps, Italy (Fig. 1). The work reports the crystal chemistry of xenotime-(Y) at this locality for the first time and adds new thortveitite crystal-chemical data to that published by Pezzotta *et al.* (2005). The minerals were investigated by electron microprobe analysis (EMPA) in wavelength-dispersive spectrometry (WDS) mode, scanning electron microscopy (SEM) in energy-dispersive spectrometry (EDS) mode, and single-crystal X-ray diffraction. A

* E-mail: fabrizio.nestola@unipd.it
DOI: 10.1180/minmag.2012.076.3.23

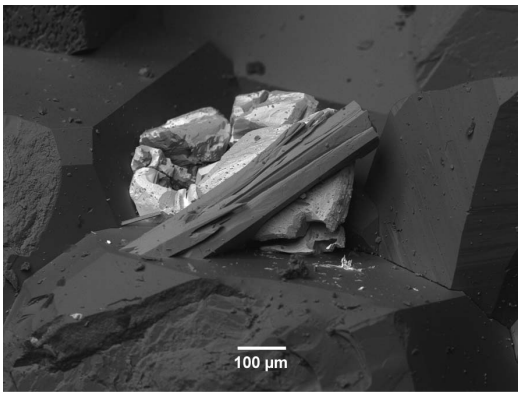

FIG. 1. A BSE image of thortveitite (platy prismatic crystal) intergrown with xenotime-(Y) (the bipyramidal crystals beneath thortveitite).

recent set of analyses of thortveitite, associated with xenotime-(Y), from this occurrence, have high SnO_2 contents (Guastoni and Nestola, 2010). Elevated SnO_2 contents in thortveitite have also been reported by Raade *et al.* (2004); they reach 5.6 wt.% in crystals from miarolitic cavities in the Heftetjern granitic pegmatite in Norway.

This work describes the partial dissolution of xenotime-(Y) and subsequent crystallization of Sn-rich thortveitite in the miarolitic cavity. The role of supercritical fluids during dissolution of xenotime-(Y) and crystallization of Sn-rich thortveitite is discussed. Detailed studies of such systems provides insights into natural processes in systems that are difficult to reproduce in laboratory experiments.

Geological sketch of the Baveno granite

The Baveno pink and white granites have been extensively quarried for ornamental purposes from the eighteenth century (Barzan, 1853). The late-Hercynian Baveno magmatic intrusion in the Western-Southern Alps is characterized by multiple intrusions, which are grouped in the Laghi Granite series (Boriani *et al*., 1988, 1995). These are small- to medium-sized granitic plutons (including the Montorfano, Baveno-Mottarone and Alzo-Roccapietra granites), with a metaluminous calc-alkaline character. They are enriched in large ion lithophile elements, suggesting a hybrid nature for their parental melts (Pinarelli *et al.*, 2002). The magmas that formed the Laghi Granites are the products of combined assimilation fractional crystallization of mantle-derived hybrid magmas residing at the base of the crust (Stille and Buletti, 1987; Pinarelli *et al*., 2002). The best estimates of the age Laghi Granites from Rb–Sr whole-rock studies are 277±8 Ma (Pinarelli *et al*., 1988) and 276±7 Ma (Schaltegger and Brack, 2007). The Baveno granite contains pegmatite pockets and miarolitic aplite/pegmatite dykes, most commonly in the pink granite. The pockets and cavities contain accessory minerals including fluorite, fluorapatite, fluorine-rich annite and siderophyllite, gadolinite-group minerals and a number of Nb-, Ta- and Y-bearing oxides. These minerals allow the pegmatites to be classified in the NYF (niobium, yttrium, fluorine) family of the miarolitic rare earth element (MI-*REE*) subclass (Pezzotta *et al.*, 1999; Černý and Ercit, 2005).

Experimental

Backscattered-electron (BSE) images of Sn-rich thortveitite and xenotime-(Y) were collected on a Jeol 5600 LV instrument at the Museo di Storia Naturale di Milano at 20 keV under low vacuum conditions (15 Pa). The chemical compositions of xenotime-(Y) and Sn-rich thortveitite were determined using a Cameca-Camebax SX50 electron microprobe operating in WDS mode at an accelerating voltage of 20 kV, current of 20 nA, with a ~1 µm beam diameter, and with 10 and 5 s counting times on the peak and background, respectively. These data were converted to oxide wt.% using the *PAP* correction program supplied by Cameca (Pouchou and Pichoir, 1985).

The following standards, lines and analysing crystal were used: wollastonite (Si$K\alpha$, Ca$K\alpha$: TAP); corundum (Al$K\alpha$; TAP); apatite (P$K\alpha$: TAP); Fe_2O_3 (Fe$K\alpha$: LiF), $MnTiO_3$ (Mn$K\alpha$: LiF); $ScPO_4$ (Sc$K\alpha$: PET); Zr-Y-*REE*-silicates (Zr$L\alpha$, Y$L\alpha$, *REEL*α and Nd$L\beta$: LiF), UO_2 and ThO_2 (U$M\alpha$ and Th$M\alpha$: PET), Nb (Nb$L\alpha$: PET). The elements Ca, Ce, Hf, La, Mg, Pb and U were sought but found to be below the experimental detection limits.

Lattice parameter determinations were performed by single-crystal X-ray diffraction using a STOE STADI-IV four-circle diffractometer equipped with a CCD detector. The sample–detector distance was 60 mm and graphite-monochromated Mo$K\alpha$ radiation was used at 50 kV and 40 mA. The crystal sizes were $0.13 \times 0.10 \times 0.07$ mm and $0.11 \times 0.08 \times 0.06$ mm for thortveitite and xenotime-(Y), respectively.

Occurrence and mineral chemistry

The specimen used for this study is from the collection of the Galerie de Minéralogie et de Géologie of the Muséum National d'Histoire Naturelle in Paris. The sample investigated is one of several studied by AG under a European 'Synthesys' project devoted to the study of Baveno minerals in European museum mineral collections.

Platy prismatic Sn-rich thortveitite crystals, up to 600 μm in size, are intergrown with xenotime-(Y) on the specimen (Fig. 1). The xenotime-(Y) occurs as bipyramidal crystals up to 500 μm long, which have corroded bipyramidal faces produced by dissolution (Fig. 2). Both minerals occur in a miarolitic cavity in laminated pale blue albite, which forms part of an aplite/pegmatite vein in the pink granite. Associated minerals include hingganite-(Y), fluorite, albite, quartz, K-feldspar, kristiansenite (Guastoni and Pezzotta, 2004) and Sn-rich ixiolite.

Backscattered-electron images of polished fragments of xenotime-(Y) and Sn-rich thortveitite show that the xenotime-(Y) is chemically homogeneous whereas the Sn-rich thortveitite is zoned from core to rim. The electron-microprobe analyses of xenotime-(Y) are reported in Table 1. Xenotime-(Y) from Baveno is particularly rich in gadolinium, with the largest amount of any xenotime from the pegmatites and hydrothermal fissures of the Alps and the Southern Alps (Demartin *et al*., 1991).

The electron-microprobe analyses of Sn-rich thortveitite (Table 1) show that the compositions of the core and rim of crystal are different. At the core, compositions are in the range 40.60–42.10 wt.% Sc_2O_3, 3.60–6.10 wt.% Y_2O_3, 2.78–3.20 wt.% SnO_2, 1.48–2.28 wt.% $Fe_2O_{3(calc)}$, and 1.28–1.73 wt.% MnO. The Gd_2O_3, Dy_2O_3 and Er_2O_3 contents are 0.12–0.18 wt.% REE_2O_3, and Yb_2O_3 is in the range of 0.39–0.59 wt.%. The total REE_2O_3 content of the Baveno thortveitite is less than the REE_2O_3 contents of thortveitite from several localities reported by Bianchi *et al*. (1988)

Scandium is significantly enriched in the rim of the crystal (at up to 45.01 wt.% Sc_2O_3) whereas Y_2O_3 falls to as little as 1.59 wt.% and Sn reduces slightly to 2.01 wt.% SnO_2. The heavy *REE* in Sn-rich thortveitite display variation with the highest Gd, Dy, Er and Yb values being found at the core of the crystal. The Sn content of up to 3.20 wt.% SnO_2 has not been reported previously in thortveitite from this locality (Pezzotta *et al.*, 2005).

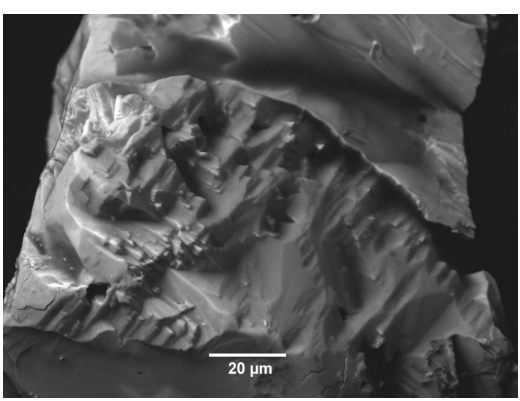

FIG. 2. A BSE image showing a partially dissolved bipyramidal crystal face of xenotime-(Y).

X-ray diffraction data

Single-crystal X-ray diffractometry was used to identify the two phases in the miarolitic cavity as thortveitite and xenotime-(Y). In the following discussion we show that the unit-cell dimensions of thortveitite (e.g. Bianchi *et al.*, 1988; this work) can be used as a preliminary indication of the Sc, Y and Yb content of the mineral, but a similar approach cannot be used for xenotime-(Y), which does not show significant changes in its unit-cell dimension if *REE*s substitute for Y. This observation is in agreement with the very small differences in the cation radii of the *REE*s.

Thortveitite

The unit-cell data for thortveitite are similar to those published by Bianchi *et al.* (1988) on their sample number 4. Bianchi *et al.* (1988) investigated thortveitite specimens from the Setesdal district in Norway and Befano in Madagascar. Each of these samples had a unit-cell volume that could be related to the Y-Sc-Yb content; unit-cell volumes of 262.4, 257.9 and 257.9 $Å^3$, were reported for samples 1, 2 and 3 respectively, with Y_2O_3 ranging from 8.4–17.7 wt.%, Sc_2O_3 from 25–27 wt.% and Yb_2O_3 from 2.6–7 wt.%. The unit-cell volume of sample 4 was significantly smaller (254.0 $Å^3$) and this sample had the highest Sc_2O_3 content (47.8 wt.%) and contained very little Y_2O_3 (2.31 wt.%) and Yb_2O_3 (0.18 wt.%). X-ray diffraction data for thortveitite and

TABLE 1. Representative chemical analyses of thortveitite and xenotime-(Y) from Baveno.

Thortveitite (wt.%)					Xenotime-(Y) (wt.%)		
	Rim	Range	Core	Range			Range
Al_2O_3	0.26	0.20–0.31	0.27	0.22–0.35	SiO_2	0.27	0.26–0.32
SiO_2	45.26	43.71–45.60	43.46	42.33–43.82	P_2O_5	35.31	34.19–37.40
Sc_2O_3	44.61	43.19–45.01	41.85	40.60–42.10	Y_2O_3	44.99	44.40–45.74
MnO	1.49	1.28–1.73	1.50	1.30–1.56	Nd_2O_3	0.24	0.15–0.48
Fe_2O_3*	1.90	1.48–2.28	1.54	1.34–1.63	Sm_2O_3	0.95	0.89–1.25
Y_2O_3	1.71	1.59–2.47	4.78	3.60–6.10	Gd_2O_3	4.18	3.61–4.77
ZrO_2	0.14	0.10–0.19	0.12	0.05–0.18	Dy_2O_3	4.33	4.03–5.36
Nb_2O_5	0.06	0.05–0.10	0.07	0.05–0.09	Ho_2O_3	0.89	0.71–1.22
SnO_2	2.54	2.01–3.07	2.98	2.78–3.20	Er_2O_3	3.10	2.82–3.22
Gd_2O_3	0.18	0.11–0.23	0.36	0.25–0.45	Yb_2O_3	4.31	3.86–4.70
Dy_2O_3	0.17	0.10–0.22	0.34	0.10–0.52	ThO_2	0.53	0.44–0.73
Er_2O_3	0.12	0.10–0.20	0.31	0.19–0.41	Total	99.10	
Yb_2O_3	0.48	0.37–0.59	0.74	0.59–0.87			
Total	98.92		98.32				
	Formula based on 7 oxygen atoms				Formula based on 4 oxygen atoms		
Si	2.021		1.997		Si	0.009	
Al	0.014		0.015		P	0.996	
Σ*T*	2.035		2.012		Σ*T*	1.005	
Sc	1.736		1.676				
Mn	0.056		0.058				
Fe^{3+}	0.064		0.053		Y	0.798	
Y	0.041		0.117		Nd	0.003	
Zr	0.003		0.003		Sm	0.011	
Nb	0.001		0.001		Gd	0.046	
Sn	0.045		0.055		Dy	0.046	
Gd	0.003		0.005		Ho	0.009	
Dy	0.002		0.005		Er	0.032	
Er	0.002		0.004		Yb	0.044	
Yb	0.007		0.010		Th	0.004	
Σ*O*	1.960		1.987		Σ*O*	0.993	

* The Fe_2O_3 value is calculated from FeO total.

xenotime-(Y) from Baveno gave the following unit-cell parameters: a = 6.528(2), b = 8.500(2), c = 4.684(1) Å, β = 102.87(3)° with V = 253.38(13) $Å^3$ for thortveitite; and a = 6.888(1), c = 6.030(1) Å with V = 286.09(8) $Å^3$ for xenotime-(Y).

The sample of thorveitite described in this study has a different chemical composition to sample 4 of Bianchi *et al.* (1988) but the unit-cell volumes are very similar [253.4 $Å^3$ of our sample compared to 254.0 $Å^3$ for that of Bianchi *et al.* (1988)]. Our measurements on the Sn-rich thortveitite from Baveno support the observation that an increasing Sc_2O_3 content (if the Y_2O_3 and Yb_2O_3 contents remain low) causes a reduction in the unit-cell volume. This is due to the larger ionic radii of Y and Yb compared to Sc (Shannon, 1976). The presence of up to 3.20 wt.% SnO_2 in thortveitite ($^{VI}Sn^{4+}$ is slightly larger than $^{VI}Sc^{3+}$) appears to have little effect on the unit-cell volume; the relatively small Sn content is insufficient to produce an obvious $^{VI}Sn^{4+}$-related volume change.

The charge imbalance produced by the incorporation of Sn^{4+} into the thortveitite structure appears to be compensated by Mn^{2+}; the mean MnO content is ~1.5 wt.% (Table 1). In our thortveitite it seems likely that a coupled substitution of the form $SnO_2 + MnO \leftrightarrow Sc_2O_3 + Y_2O_3$ occurs. This substitution mechanism is

supported by previous work in which significant amounts of Zr^{4+} in thortveitite were found to be charge balanced by Mn^{2+}, Ca^{2+} and Mg^{2+} (Bianchi *et al*., 1988)

Xenotime-(Y)

Mogilevsky *et al.* (2006) compared the unit-cell dimensions of several synthetic xenotime-type structures with natural xenotime-(Y) crystals from Novo Horizonte in Brazil and found that synthetic YPO_4 has a unit cell that is practically indistinguishable from the Brazilian samples. Although the natural xenotime-(Y) studied by Mogilevsky *et al.* (2006) has a composition in which 24 mol.% Y is replaced by other *REE* cations, the difference in the *a* and *c* unit-cell parameters compared to synthetic xenotime-(Y) is extremely small, with $a = 6.898$ and $c = 6.037$ Å for the natural Novo Horizonte xenotime-(Y), compared to $a = 6.883$ and $c = 6.021$ Å (Ushakov *et al.*, 2001) and $a = 6.884$ and $c = 6.020$ Å (Aldred, 1984) for synthetic YPO_4. Further comparisons can be made with xenotime-(Y) from granitic rocks at Nanling, southeast China (Ni *et al.*, 1995). This has a composition which contains 77 mol.% Y, the remaining 23 mol.% being almost entirely other *REE* cations; the unit-cell dimensions are $a = 6.895(1)$ and $c = 6.027(1)$ Å, which is also extremely close to synthetic xenotime.

The natural sample of xenotime-(Y) from Baveno described here has unit-cell dimensions $a = 6.888(1)$ and $c = 6.030(1)$ Å and ~20 mol.% *REE*s substituting for Y. Thus our data confirm the observation that this level of substitution of *REE* cations for Y does not alter the unit-cell dimensions of xenotime significantly.

Crystallization processes in the miarolitic cavities at Baveno: the role of fluids

The granitic pegmatites at Baveno contain millimetre- to centimetre-sized miarolitic cavities, which represent unique relatively well-sealed geochemical environments. Crystallization of the pegmatites begins from silicate liquids. As the melts cool, the high concentrations of B, F, P and H_2O, in the melt lead to a transition which produces silicate melt and a coexisting supercritical aqueous fluid (London, 1987, 1992, 1997, 2005). Incompatible elements including tin, scandium, yttrium and *REE*s partition into the silicate liquid melt and contribute to the formation of the rare accessory phases that are characteristic of pegmatites. At Baveno these include the miarolitic cavity minerals xenotime-(Y) and thortveitite.

The xenotime-(Y) crystals are corroded (Fig. 2) but the thortveitite crystals have plane crystal faces with a vitreous lustre. The thortveitite at Baveno commonly has incipient reaction border zones; the crystals are usually opaque and are covered by other phases including *REE*-bearing carbonates (Gramaccioli *et al.*, 2000*a*; Pezzotta *et al.*, 2005).

Crystallization processes are controlled by factors including the kinetics of nucleation, adsorption and diffusion of elements along the fluid–crystal interfaces, saturation, temperature and pressure in fluids. Taking these into consideration it can be assumed that the crystallization and growth of xenotime-(Y) started in a geochemical environment controlled by low ΔT undercooling and supersaturation of SiO_2 (London *et al.*, 1999).

After the xenotime-(Y) crystallized, it was partially dissolved, with the major dissolution affecting the bipyramidal crystals faces (Fig. 2). The corrosion mechanism can be probably be best represented using a dissolution reaction at low pH such as $YPO_4 + 3H^+ \rightarrow Y^{3+} + H_3PO_4$ (Cetiner *et al.*, 2005; Liu and Byrne, 1997). Assuming a pure endmember Y-phosphate, the reaction is controlled by the solubility product $K_{s0} = a_{Y^{3+}}a_{PO_4^{3-}}$; unfortunately, experimental solubility data at high temperatures are still lacking for almost all *REE*-bearing minerals (Cetiner *et al*., 2005). At this stage aggressive supercritical fluids probably liberated the yttrium that was incorporated into the thortveitite crystals.

Experimental studies at different temperatures support the role of complexing agents such as fluoride, chloride, sulfate, carbonate and hydroxide ions in the transportation of *REE*s, yttrium and scandium in supercritical fluids (Kosterin, 1959; Bilal *et al*., 1987; Wood, 1990). In miarolitic pegmatites, fluorine and carbonate are the best candidates as complexing agents for Y and *REE* (Gramaccioli *et al.*, 2000*b*; Wood, 1990). Fluorine plays an important role in the enrichment of tin, scandium, yttrium and *REE*s in supercritical and high-temperature hydrothermal aqueous fluids (London, 1987; Keppler, 1993).

The source of the Y and *REE* in the supercritical fluids at Baveno is likely to be mica-group minerals and related sheet silicates. These minerals behave like a sponge, and incompatible elements are commonly incorporated in their

structures. Indeed, annite-siderophyllite and chamosite are widespread at Baveno, the former in the granite and the latter lining miarolitic cavities, where they commonly show incipient alteration (Guastoni, 2012).

Conclusions

Thortveitite from miarolitic cavities at Baveno contains up to 3.20 wt.% SnO_2. Xenotime-(Y) from Baveno is enriched in the gadolinium in comparison to specimens from other pegmatites and hydrothermal fissures of the Alps and Southern Alps. The unit-cell parameters of thortveitite can be used as preliminary indicators of its Sc_2O_3, Y_2O_3, Yb_2O_3 content, but a similar approach cannot be used for xenotime-(Y), as it does not show significant differences in unit-cell size as a function of substitution. Thortveitite and xenotime-(Y) are found in miarolitic cavities where they illustrate late-stage dissolution and crystallization processes. The source of the Y and *REE*s is probably the alteration of sheet silicates (annite-siderophyllite and chamosite) by supercritical aqueous fluids.

Acknowledgements

We are indebted to the Synthesys project FR-TAF-78 that provided financial support for this study. We would like also to thank Dr Federico Pezzotta of the Museum of Natural History of Milan who facilitated the use of the SEM-EDS microscope and David London for his valued contributions.

References

Aldred, A.T. (1984) Cell volumes of APO_4, AVO_4, and $ANbO_4$ compounds, where A = Sc, Y, La–Lu. *Acta Crystallographica*, **B40**, 569–574.

Barzan, G. (1853) Il granito di Baveno. *Giornale del Regio Istituto Lombardo di Scienze, Lettere e Arti, Milano*, **23**, 417–433.

Bianchi, R., Pilati, T., Diella, V., Gramaccioli, C.M. and Mannucci, G. (1988) A re-examination of thortveitite. *American Mineralogist*, **73**, 601–607.

Bilal, B.A. and Langer, P. (1987) Complex formation of trace elements in geochemical systems: stability constants of fluoro complexes of the lanthanides in a fluorite bearing model system up to 200ºC and 1000 bar. *Inorganica Chimica Acta*, **140**, 297–298.

Boriani, A., Caironi, V., Oddone, M. and Vannucci, R. (1988) Some petrological and geochemical constraints on the genesis of the Baveno-Mottarone and Montorfano plutonic bodies. *Rendiconti Società Italiana di Mineralogia e Petrologia*, **43**, 385–394.

Boriani, A., Giobbi Origoni, E. and Pinarelli L. (1995) Paleozoic evolution of southern Alpine crust (northern Italy) as indicated by contrasting granitoid suites. *Lithos*, **35**, 47–63.

Ćerný P. and Ercit, S. (2005). The classification of granitic pegmatites revisited. *The Canadian Mineralogist*, **43**, 2005–2026.

Cetiner, Z.S., Wood, S.A. and Gammons, C.H. (2005) The aqueous geochemistry of the rare earth elements. Part XIV. The solubility of rare earth element phosphates from 23 to 150ºC. *Chemical Geology*, **217**, 147–169.

Demartin, F., Pilati, T., Diella, V., Donzelli, S., Gentile, P. and Gramaccioli, C.M. (1991) The chemical composition of xenotime from fissures and pegmatites in the Alps. *The Canadian Mineralogist*, **29**, 69–75.

Gramaccioli, C.M., Diella, V., Demartin, F., Orlandi, P. and Campostrini, I. (2000*a*) Cesian bazzite and thortveitite from Cuasso al Monte, Varese, Italy: a comparison with the material from Baveno, and inferred origin. *The Canadian Mineralogist*, **38**, 1409–1418.

Gramaccioli, C.M., Diella, V. and Demartin, F. (2000*b*) The formation of scandium minerals as an example of the role of complexes in the geochemistry of rare earths and HFS elements. *European Journal of Mineralogy*, **12**, 795–808.

Guastoni, A. (2012) *LCT (Lithium, Cesium, Tantalum) and NYF (Niobium, Yttrium, Fluorine) pegmatites in the Central Alps. Proxies of exhumation history of the Alpine nappe stack in the Lepontine dome*. Unpublished PhD Thesis, XXIV cycle, University of Padova, Padova, Italy.

Guastoni, A. and Nestola, F. (2010) Sn-rich thortveitite intergrowth with xenotime-(Y): Y versus Sc fractionation in NYF miarolitic pegmatites at Baveno (Southern Alps, Italy). *Acta Mineralogica-Petrographica*, 20th General Meeting, IMA, Budapest, Ungheria, Abstract Volume **6**, 616.

Guastoni, A. and Pezzotta, F. (2004) Kristiansenite a Baveno, secondo ritrovamento mondiale della specie. *Rivista Mineralogica Italiana*, **30**, 247–251.

Guastoni, A., Nestola, F. and Giaretta, A. (2009) Mineral chemistry and alteration of rare earth element (*REE*) carbonates from alkaline pegmatites of Mount Malosa, Malawi. *American Mineralogist*, **94**, 1216–1222.

Hsu, L.C. (1992) Synthesis and stability of bastnaesites in a part of the system (Ce,La)–F–H–C–O. *Mineralogy and Petrology*, **47**, 87–101.

Keppler, H. (1993) Influence of fluorine on the enrichment of high field strength trace elements in

granitic rocks. *Contributions to Mineralogy and Petrology*, **114**, 479–488.

Kosterin, A.V. (1959) The possible modes of transport of the rare earths by hydrothermal solutions. *Geochemistry International*, **4**, 381–387.

Liu, X. and Byrne, R.H. (1997) Rare earth and yttrium phosphate solubilities in aqueous solution. *Geochimica et Cosmochimica Acta*, **61**, 1625–1633.

London, D. (1987) Internal differentiation of rare-element pegmatites: effects of boron, phosphorous, and fluorine. *Geochimica et Cosmochimica Acta*, **51**, 403–420.

London, D (1992) The application of experimental petrology to the genesis and evolution of granitic pegmatites. *The Canadian Mineralogist*, **30**, 499–540.

London, D. (1997) Estimating abundances of volatile and other mobile components in evolved silicic melts through mineral–melt equilibria. *Journal of Petrology*, **38**, 1691–1706.

London, D. (2005) Granitic pegmatites: an assessment of current concepts and directions for the future. *Lithos*, **80**, 201–303.

London, D. (2008) *Pegmatites*. Canadian Mineralogist Special Publication **10**. Mineralogical Association of Canada, Québec, Canada, 347 pp

London, D., Wolf, M.B., Morgan, G.B. VI and Garrido M.G. (1999) Experimental silicate–phosphate equilibria in peraluminous granitic magmas, with a case study of the Alburquerque batholith at Tres Arroyos, Badajoz, Spain. *Journal of Petrology*, **40**, 215–240.

Mogilevsky, P., Zaretsky, E.B., Parthasarathy, T.A. and Meisenkothen, F. (2006) Composition, lattice parameters, and room temperature elastic constants of natural single crystal xenotime from Novo Horizonte. *Physics and Chemistry of Minerals*, **33**, 691–698.

Ni, Y., Hughes, J.M. and Mariano, A.N. (1995) Crystal chemistry of the monazite and xenotime structures. *American Mineralogist*, **80**, 21–26.

Pezzotta, F., Diella, V. and Guastoni, A. (1999) Chemical and paragenetic data on gadolinite-group minerals from Baveno and Cuasso al Monte, southern Alps, Italy. *American Mineralogist*, **84**, 782–789.

Pezzotta, F., Diella V. and Guastoni, A. (2005) Scandium silicates from Baveno and Cuasso al Monte NYF-granites, Southern Alps (Italy). Mineralogy and genetic inferences. *American Mineralogist*, **90**, 1442–1452.

Pinarelli, L., Del Moro, A. and Boriani, A. (1988) Rb-Sr Geochronology of Lower Permian plutonism in Massiccio dei Laghi, Southern Alps (NW Italy). *Rendiconti Società Italiana di Mineralogia e Petrologia*, **43**, 411–428.

Pinarelli, L., Del Moro, A., Boriani, A. and Caironi, V. (2002) Sr, Nd isotope evidence for an enriched mantle component in the origins of the Hercynian gabbro-granite series of the "Serie dei Laghi" (Southern Alps, NW Italy). *European Journal of Mineralogy*, **14**, 403–415.

Pouchou, J.L. and Pichoir, F. (1985) 'PAP' $\varphi(\rho Z)$ procedure for improved quantitative microanalysis. Pp. 104–106 in: *Microbeam Analysis* (J.T. Armstrong, editor). San Francisco Press, San Francisco, California, USA.

Raade, G., Bernhard, F. and Ottolini, L. (2004) Replacement textures involving four scandium silicate minerals in the Heftetjern granitic pegmatite, Norway. *European Journal of Mineralogy*, **16**, 945–950.

Schaltegger, U. and Brack, P. (2007) Crustal-scale magmatic systems during intracontinental strike-slip tectonics: U, Pb and Hf isotopic constraints from Permian magmatic rocks of the Southern Alps. *International Journal of Earth Sciences*, **96**, 1131–1151.

Shannon, R.D. (1976) Revised effective ionic radii and systematic studies of interatomic distances in halides and chalcogenides. *Acta Crystallographica*, **A32**, 751–767.

Stille, P. and Buletti, M. (1987) Nd-Sr isotopic characteristics of the Lugano volcanic rocks and constraints on the continental crust formation in the South Alpine domain (N. Italy-Switzerland). *Contributions to Mineralogy and Petrology*, **96**, 140–150.

Ushakov, S.V., Helean, K.B., Navrotsky, A. and Boatner, L.A. (2001) Thermochemistry of rare-earth orthophosphates. *Journal of Materials Research*, **16**, 2623–2633.

Wood, S. A. (1990) The aqueous geochemistry of the rare-earth elements and yttrium 2. Theoretical predictions of speciation in hydrothermal solutions to 350ºC at saturation water vapour pressure. *Chemical Geology*, **88**, 99–125.